Solid-State Polycondensation of Poly(ethylene terephthalate): Kinetics and Mechanism

TANG ZHI-LIAN,[1,*] QIU GAO,[1] HUANG NAN-XUN,[1] and CLAUDIO SIRONI[2]

[1]Chemical Engineering, China Textile University, 1882 West Yan-An Road, Shanghai, 200051, Peoples Republic of China and [2]Noyvallesina Engineering, SpA Via Sant'Aberto, 1, 24020 Parre (BG), Italy

SYNOPSIS

A numerical method to seek a solution for the solid-state polycondensation (SSP) process has been proposed to analyze the mechanism of SSP. Results expound that, for the industrial SSP process of PET, the overall reaction rate in a single pellet is appropriately simulated by the diffusion and reaction rate jointly controlling the model. From the core to the surface the SSP rate increases monotonically due to a gradual reduction of the concentration of such by-products as ethylene glycol and water. However, the SSP rate at any location within the pellet is constrained between two purely reaction rate controlling cases. © 1995 John Wiley & Sons, Inc.

INTRODUCTION

For preparing poly(ethylene terephthalate) (PET) with molecular weight greater than 20,000 suitable for industrial textile applications, solid-state polycondensation (SSP) is generally preferred.[1-4] SSP is carried out by heating the low molecular weight polymer pellets at a temperature below their melting temperature but above their glass transition temperature. The polymer, at a reaction temperature of 200–240°C, which is much lower than that for the melt polymerization process thereby significantly depressing the thermal degradation, is further condensed and the molecular weight increased with the by-products removed by applying vacuum or flushing with inert gas.

Extensive work has been reported on the experimental study of the factors affecting the SSP of PET. Various authors have investigated the mechanism of the process by means of diverse models. For example, Chang[2] interpreted his data using a diffusion model, whereas Shaaf et al.[3] and Chen et al.[4] analyzed their data using a purely kinetic model. Thereafter, Ravindranath and Mashelkar[5] developed a comprehensive model where, under certain assumptions, either a diffusion model or a kinetic model may be derived. They assumed that the main polycondensation reaction is an equilibrium reaction. The removal of by-products, predominantly ethylene glycol (EG), will favor the forward reaction considerably.

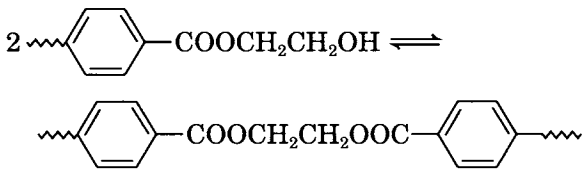

$$+ \mathrm{HOCH_2CH_2OH} \quad (1)$$

$$2E \rightleftharpoons Z + \mathrm{EG}. \quad (2)$$

Obviously, the polycondensation rate of SSP, as a whole, depends on both chemical reaction and physical diffusion of EG through the pellet. In their diffusion and reaction controlling model, the one-dimensional (1-D) unsteady state diffusion process of EG, coupled with the time rate change of the polymer end-group concentration in a single particle is described by the following governing equations:

$$\frac{\partial g}{\partial t} = D_1 \frac{\partial^2 g}{\partial x^2} - \frac{1}{2}\frac{\partial e}{\partial t} \quad (3)$$

$$\frac{\partial e}{\partial t} = -2k_1\left(e^2 - \frac{4gz}{K_1}\right) \quad (4)$$

* To whom correspondence should be addressed.

Journal of Applied Polymer Science, Vol. 57, 473–485 (1995)
 CCC 0021-8995/95/040473-13

$$z = z_o + \frac{e_o - e}{2} = 1 - \frac{e}{2} \tag{5}$$

where e, z, and g are the concentrations of hydroxyl end groups, diester groups, and EG, respectively. D_1 is the diffusivity of EG, K_1 and k_1 are the equilibrium and forward rate constants of the ester interchange reaction, with the initial and boundary conditions

$$g = g_o, \quad e = e_o, \quad z = z_o, \quad t = 0, \quad 0 \le x \le x_o \tag{6}$$

$$g = g_s, \quad \frac{\partial e}{\partial x} = 0, \frac{\partial z}{\partial x} = 0, \quad t > 0, \quad x = x_o \tag{7}$$

or

$$-D_1 \frac{\partial g}{\partial x} = k_g(g - g_b), \quad \frac{\partial e}{\partial x} = 0, \quad \frac{\partial z}{\partial x} = 0, \quad t > 0, \quad x = x_o \tag{8}$$

$$\frac{\partial g}{\partial x} = 0, \quad \frac{\partial e}{\partial x} = 0, \quad \frac{\partial z}{\partial x} = 0, \quad t > 0, \quad x = 0 \tag{9}$$

where g_s and g_b are the concentrations of EG at the gas–solid interface and in the bulk of the inert gas phase, k_g is the gas-phase mass transfer coefficient. Generally SSP is carried out under very high vacuum or high inert gas flow rate, so that the mass transfer resistance in the gaseous phase is negligible, i.e. $g_s = g_b$. In connection with this, boundary condition (8) reduces to (7) spontaneously.

If the diffusion of EG is so rapid that the concentration of EG can be assumed to be nearly zero throughout the particle, the reaction is purely chemical reaction rate controlled. Then eq. (4) is reduced to

$$\frac{de}{dt} = -2k_1 e^2. \tag{10}$$

Applying eq. (10) to the data of Chen et al.,[4] they evaluated k_1 at 160°C to be 0.1172 (mol/⟨⬡⟩)$^{-1}$ h^{-1}, which is surprisingly close to the value of 0.1170 (mol/⟨⬡⟩)$^{-1}$ h^{-1}, from the data on melt polycondensation reported by Yokoyama et al.,[6] with its activation energy equal to 18.5 kcal/mol.

When the rate of polycondensation reaction is much faster than the diffusion of EG, the SSP should be governed by a diffusion controlled process. The reaction was then assumed to be at equilibrium at all points and the following relation holds:

$$e^2 = \frac{4gz}{K_1}. \tag{11}$$

Given this relation *a priori*, substituting the derivative of eq. (11) into eq. (3), Ravin Dranath et al. analyzed the experimental data of Chang[2] and evaluated D_1, diffusivity of EG, as 3.6×10^{-6} cm^2/s at 230°C with its activation energy equal to 31.26 kcal/mol. Figures indicating the activation energy of diffusivity much higher than 18.5 kcal/mol, the activation energy of the forward rate constant, may imply that the decrease of diffusion rate of EG due to a decrease of temperature should be faster than the decrease of the reaction rate. Therefore the lower the reaction temperature, the less credible it would be to employ the reaction rate controlling model to explain the results. However, following previous work, they found the data at as low as 160°C in good agreement with a reaction rate controlled process and treated the data at higher temperatures as from a diffusion controlled process. This apparent discrepancy may entail some sort of suspicion on the choice of the values of activation energies for simulation parameters. Nevertheless, there have been diversified values of diffusion activation energies reported, such as 5.4 kcal/mol by Chen and Chen.[7] Further, because polymer end groups are confined in the solid state and recognized as not subject to Fickian diffusion, it seems redundant to include the following boundary conditions in eqs. (7) and (9)

$$\frac{\partial e}{\partial x} = 0, \quad \frac{\partial z}{\partial x} = 0, \quad t > 0, \quad x = x_o, \quad x = 0$$

to keep both z and e from diffusing across the boundary. In particular, we come to a similar conclusion by inspecting the order of the variable e or z in the governing differential equations. Insofar as it is involved in the first derivative of time only, an initial condition should be sufficient for a unique solution.

Further, the said models completely ignore the esterification moiety, which is inconsistent with the fact that, when the —COOH content is not low enough, the esterification reaction as well as the diffusion of water must also be considered. On the basis of the foregoing, we take into account both chain extension polycondensation reactions and propose a numerical method to seek a solution for the SSP process in a 1-D model, which can be subsequently extended to a 3-D model for different particle sizes and shapes. The objective of the present work is to

provide a set of solutions that describe the process and concentration profiles inside the particle thereby generating suitable criteria for data analysis that can be utilized in designing a SSP reactor as well as in elucidating a number of lacunae that appeared in hitherto existing concepts concerning the controlling mechanism in SSP.

FUNDAMENTALS

Chain extension (polycondensation) of PET is conventionally accomplished by two reversible reactions in SSP. Besides the ester interchange reaction, eq. (1), an esterification reaction, eq. (12), occurs simultaneously.

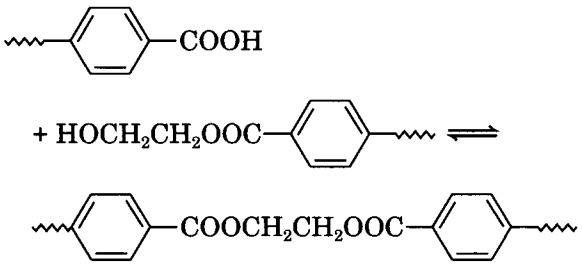

$$+ H_2O \quad (12)$$

$$C + E \rightleftharpoons Z + W. \quad (13)$$

Herein E, C, Z, EG, and W in eq. (2) and (13) may indicate implicitly hydroxyl end group —OH, carboxyl end group —COOH, diester group, by-products of EG $HOCH_2CH_2OH$, and water H_2O. Assuming that the diffusion process of EG and W is of Fickian type and isothermal without volume change of the particle, the 1-D unsteady state diffusion process coupled with the concentration change of polymer end groups can be described by eqs. (14)-(21):

$$\frac{\partial g}{\partial t} = D_1 \frac{\partial^2 g}{\partial x^2} - \frac{1}{2}\left(\frac{\partial e}{\partial t} - \frac{\partial c}{\partial t}\right) \quad (14)$$

$$\frac{\partial e}{\partial t} = -2k_1\left(e^2 - \frac{4gz}{K_1}\right) - k_2\left(ec - \frac{2wz}{K_2}\right) \quad (15)$$

$$\frac{\partial w}{\partial t} = D_2 \frac{\partial^2 w}{\partial x^2} - \frac{\partial c}{\partial t} \quad (16)$$

$$\frac{\partial c}{\partial t} = -k_2\left(ec - \frac{2wz}{K_2}\right) \quad (17)$$

$$z = z_o + \frac{(e_o + c_o) - (e + c)}{2} = 1 - \frac{e + c}{2} \quad (18)$$

The relevant boundary conditions are

$$e = e_o, \quad c = c_o, \quad g = g_o,$$
$$w = w_o, \quad t = 0, \quad 0 \le x \le x_o, \quad (19)$$

$$g = g_s, \quad w = w_s, \quad t > 0, \quad x = x_o, \quad (20)$$

$$\frac{\partial g}{\partial x} = 0, \quad \frac{\partial w}{\partial x} = 0, \quad t > 0, \quad x = 0. \quad (21)$$

Here e, c, z, g, and w are the concentrations of hydroxyl end groups, carboxyl end groups, diester groups, EG, and water, respectively. K_1, k_1, and K_2, k_2 are the equilibrium and forward rate constants of ester interchange and esterification reaction; D_1, D_2 are the diffusivity of EG and water. g_s and w_s are the concentrations of EG and W at the gas–solid interface. By virtue of transformation of variables as

$$p = t/t_f \quad (22)$$

$$q = x/x_o, \quad (23)$$

eqs. (14)-(21) are converted to eqs. (24)-(31)

$$\frac{\partial g}{\partial p} = \left(\frac{t_f}{x_0^2} D_1\right)\frac{\partial^2 g}{\partial q^2} - \frac{1}{2}\left(\frac{\partial e}{\partial p} - \frac{\partial c}{\partial p}\right) \quad (24)$$

$$\frac{\partial e}{\partial p} = -2(k_1 t_f)\left(e^2 - \frac{4gz}{K_1}\right) - (k_2 t_f)\left(ec - \frac{2wz}{K_2}\right) \quad (25)$$

$$\frac{\partial w}{\partial p} = \left(\frac{t_f}{x_o^2} D_2\right)\frac{\partial^2 w}{\partial g^2} - \frac{\partial c}{\partial p} \quad (26)$$

$$\frac{\partial c}{\partial p} = -(k_2 t_f)\left(ec - \frac{2wz}{K_2}\right) \quad (27)$$

$$z = 1 - \frac{e + c}{2} \quad (28)$$

$$e = e_o, \quad c = c_o, \quad g = g_o,$$
$$w = w_o, \quad p = 0, \quad 0 \le q \le 1 \quad (29)$$

$$g = g_s, \quad w = w_s, \quad p > 0, \quad q = 1 \quad (30)$$

$$\frac{\partial g}{\partial q} = 0, \quad \frac{\partial w}{\partial q} = 0, \quad p > 0, \quad q = 0. \quad (31)$$

Table I Influence of N_2 Flow Rate on SSP Reaction at 225°C for 30 h

Flow rate (L/min kg PET)	0.5	2.0	3.0	4.0	5.0
Intrinsic viscosity	0.953	1.057	1.071	1.069	1.070
Molecular weight ($\times 10^{-4}$)	2.881	3.269	3.322	3.315	3.318

The degree of polymerization (Pn) can be calculated from e and c as

$$Pn = \frac{2}{e + c}. \tag{32}$$

We proceed with the simulation procedure for eqs. (24)–(31) by resorting to numerical calculation. The technique for numerical calculation is a combination of the Runge–Kutta method, which deals with the time interval integration, and finite difference method, which handles the internal divisions of the particle.

EXPERIMENTAL

Materials and Sample Preparation

Commercial PET precursors were supplied by a local polyester manufacturer, prepared by a melt process. The PET pellets were 4 × 4 × 1.5 mm. Its initial intrinsic viscosity was 0.72. Before SSP, samples were vacuum dried for 12 h at 140°C to reduce the moisture concentration to less than 30 ppm to avert hydrolytic degradation during SSP.

Apparatus

The SSP was conducted in a fixed bed reactor with a heated stream of dry nitrogen gas flowing through it. The tube reactor is 2.5 cm in diameter and 300 cm long, embedded in a jacket with salt melt circulating through it. The jacket is equipped with sophisticated heating and monitoring systems to homogenize the temperature distribution in the fixed bed reactor.

Sampling

After each reaction was completed, a nitrogen purge was maintained until the fixed bed reactor was cooled to room temperature. Samples were collected by mixing the pellets taken from the upper, middle, and lower sections of the reactor. In determining the viscosity of the polymer at the surface and in the center of a pellet, material scraped from the skin and that left on the core were used.

Determination of Intrinsic Viscosity

The Intrinsic viscosities were measured using an Ubbelohde viscometer with the mixture of 1,1,2,2-tetrachloroethane and phenol (1 : 1 by volume) as solvent at 25 ± 0.02°C. Thus the $\bar{M}_n$ can be calculated from the intrinsic viscosity as

$$[\eta] = 2.1 \times 10^{-4} \bar{M}_n^{0.82} \tag{33}$$

The concentration of carboxyl end groups was determined by titration in benzyl alcohol.[9]

RESULTS AND DISCUSSION

The experimental data are tabulated in Tables I and II.

Table II Experimental Data at Various N_2 Flow Rates

Flow Rate (L/min kg PET)	Time (h)	Intrinsic Viscosity (dL/g)			Molecular Weight (g/mol)			[COOH] (μeq/g)
		Overall	Surface	Center	Overall	Surface	Center	
0.5	10	0.837			24600			16.7
	20	0.893			26620			14.7
	30	0.953			28810			13.5
2.0	10	0.859	0.887	0.837	25390	26400	24600	15.9
	20	0.963	1.039	0.935	29180	32010	28150	13.6
	30	1.057	1.141	1.007	32690	35900	30800	12.0

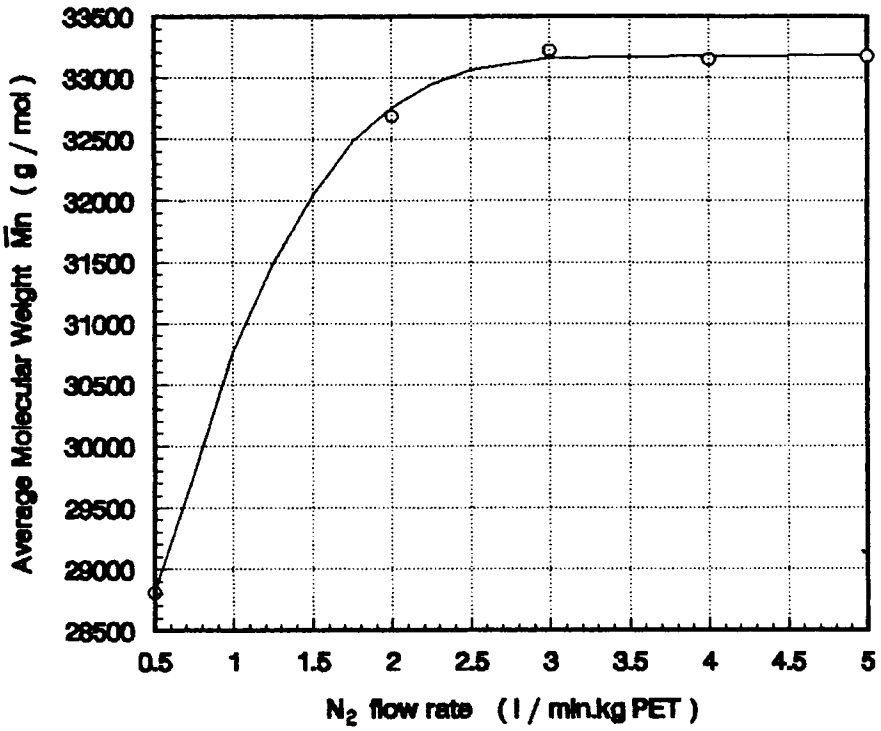

Figure 1 Influence of nitrogen gas flow rate on SSP. e_o = 0.01472, c_o = 0.00398, x_o = 0.075, reaction temp. = 225°C, reaction time t = 30 h.

Influence of Flow Rate of Inert Gas

The influence of N_2 flow rate on SSP reaction is shown on Figure 1. When all other operating conditions are the same, number average molecular weight of PET after SSP for 30 h at 225°C increases with increasing nitrogen flow rate up to a plateau. Similar results were reported by other investigators.[3,10] There appears to be a critical flow rate associated with a pair of g_s and w_s, which cease to decrease with increasing flow rate.

Diffusion and Reaction Rate Controlling Model

Collected data were processed by using a diffusion and reaction rate model with equilibrium constance[11,12] $K_1 = 1$ and $K_2 = 1.25$ to evaluate parameters D_1, D_2, k_1, k_2, g_s, and w_s. Referring to the data of the melt polycondensation rate constant[6,13] and the diffusivity of water,[14] a set of initial values of these parameters were estimated to invoke the Simplex Program for the optimum evaluation of these parameters through the best fit of experimental data with the predicted results in average $\bar{M}_n$ (Fig. 2) and the concentration of carboxyl end groups (Fig. 3). The simultaneous evaluation strategy executed here incorporates and coordinates the effects of individual evaluations of different mechanisms, such as D_1, D_2 in diffusion, k_1, k_2 in kinetics, and g_s, w_s for boundary conditions, which, when in need of high accuracy, have to be determined independently. However, the simultaneous evaluation feasible in statistics creates a comprehensible result particularly suitable for engineering interest. In Figure 2, each curve demonstrates the increase of average molecular weight vs. time at various flow rates for $D_1 = 2.6 \times 10^{-6}$ cm^2/s, $D_2 = 5.8 \times 10^{-6}$ cm^2/s, $k_1 = 1.06$ (mol/ ⬡)$^{-1}$ h^{-1}, $k_2 = 4.08$ (mol/ ⬡)$^{-1}$ h^{-1}. Higher flow rate will create smaller g_s and w_s. Curves 3 and 4 correspond, respectively, to a pair of g_s and w_s at and below the critical flow rate. Curves 1 and 2, corresponding to $g_s = 0$, $w_s = 0$, and $g_s = 9 \times 10^{-7}$, $w_s = 8 \times 10^{-7}$ (mol/ ⬡) are calculated to predict the theoretical upper limit that might be approached under very high vacuum SSP. Figures 4–8 delineate the spatial representations of hydroxyl end group, carboxyl end group, local molecular weight, EG, and water in the pellet. In Figures 7 and 8, at the edge of the reaction surface $x = 0$, the derivative of g and w with respect to x is found to vanish throughout the duration of reaction; in Figures 4 and 5, derivatives equal to zero are not observed on both boundaries as the result of omission of the superfluous boundary conditions. Curves in Figure 9 show mo-

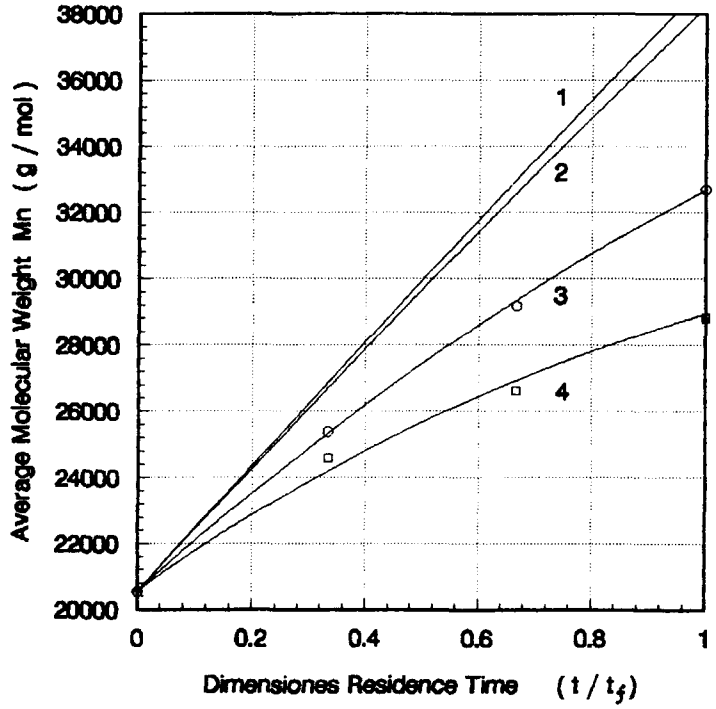

Figure 2 Average molecular weight vs. time at various N_2 flow rates, experimental data (○) and (□) correspond to N_2 flow rate of 2 and 0.5 L/min kg PET. Parameters: $D_1 = 2.6 \times 10^{-6}$, $D_2 = 5.8 \times 10^{-6}$, $k_1 = 1.06$, $k_2 = 4.08$, $K_1 = 1$, $K_2 = 1.25$, $x_o = 0.075$, $e_o = 0.01472$, $c_o = 0.00398$, $g_o = 1 \times 10^{-5}$, $w_o = 2 \times 10^{-5}$; curves 1–4 correspond to $g_s = 0$, $w_s = 0$; $g_s = 9 \times 10^{-6}$, $w_s = 8 \times 10^{-6}$; $g_s = 9 \times 10^{-7}$, $w_s = 8 \times 10^{-7}$; $g_s = 1.96 \times 10^{-5}$, $w_s = 1.28 \times 10^{-5}$, respectively.

lecular weight vs. time at various localities in the pellet, $x = 0, 1/5\ x_o, 2/5\ x_o, 3/5\ x_o, 4/5\ x_o, x_o$, from the core to the surface. It is observed that the outer part enjoys a faster rate of increase of M_n than the inner part as a result of the decrease of concentration of EG and W from inner to outer part, coinciding with the experimental data shown in Figure 9.

First Kind of Reaction Rate Controlling Model

If the concentrations of EG and W are nearly zero, eqs. (24)–(28) reduce to the eqs. (34)–(35), which represent the SSP at maximum reaction rate.

$$\frac{\partial e}{\partial p} = -2(k_1 t_f)e^2 - (k_2 t_f)(ec) \qquad (34)$$

$$\frac{\partial c}{\partial p} = -(k_2 t_f)(ec). \qquad (35)$$

M_n converted from the results of eqs. (34)–(35) by eq. (32) is plotted in Figures 9 and 10 by a broken line at the top, standing for the hypothetical maximum rate. Even the SSP occurring at the surface (curve 6 in Fig. 9 and 5 in Fig. 10), where the diffusion takes place most rapidly, does not approach it because of the insufficiently large value of D_1, D_2 and $g_s \neq 0$, $w_s \neq 0$.

Second Kind of Reaction Rate Controlling Model

In this case the diffusion of by-products of EG and W is extremely slow, such that the diffusion part can be dropped from eqs. (24) and (26). This is another kind of purely reaction rate controlling process insofar as diffusivity is not involved in the equation. In fact, this is the reaction proceeding in a closed system as if the particle were completely wrapped up. When plotted in Figure 10 by a nearly horizontal broken line at the bottom for a pellet of larger size, the result of eqs. (24)–(31), assuming D_1 and D_2 equal to zero, appears very close to curve 1, which represents the reaction rate of SSP at the core. In the core region, diffusion is recognized as the slowest because of the longest distance to reach the surface.

Diffusion Controlling Model

A unique diffusion controlling model developed by Ravindranath and Masheldar,[5] which is concomi-

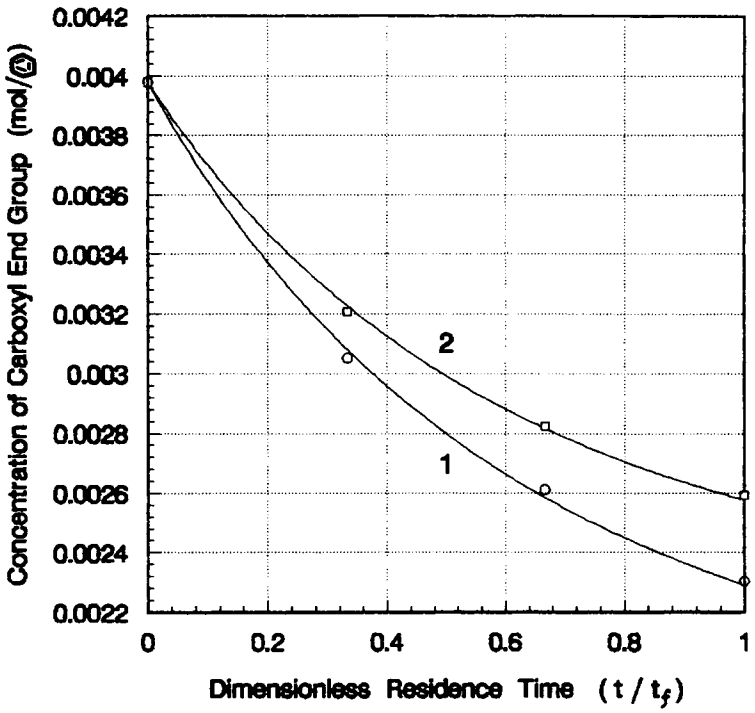

Figure 3 Concentration of carboxyl end group in a pellet vs. time during SSP at 225°C. Experimental data (○) and (□) correspond to N_2 flow rate of 2 and 0.5 L/min kg PET. The parameters of curves 1 and 2 are the same as those of curves 3 and 4 in Figure 2.

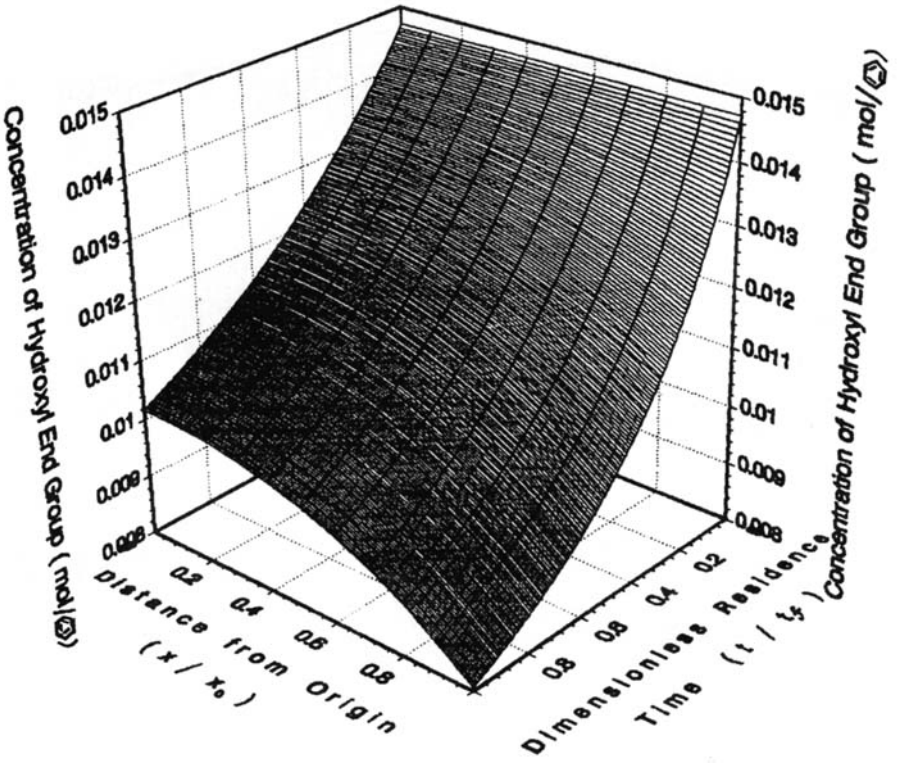

Figure 4 Internal distribution of hydroxyl end group in a pellet during SSP at 225°C. The parameters are the same as those of curve 3 in Figure 2.

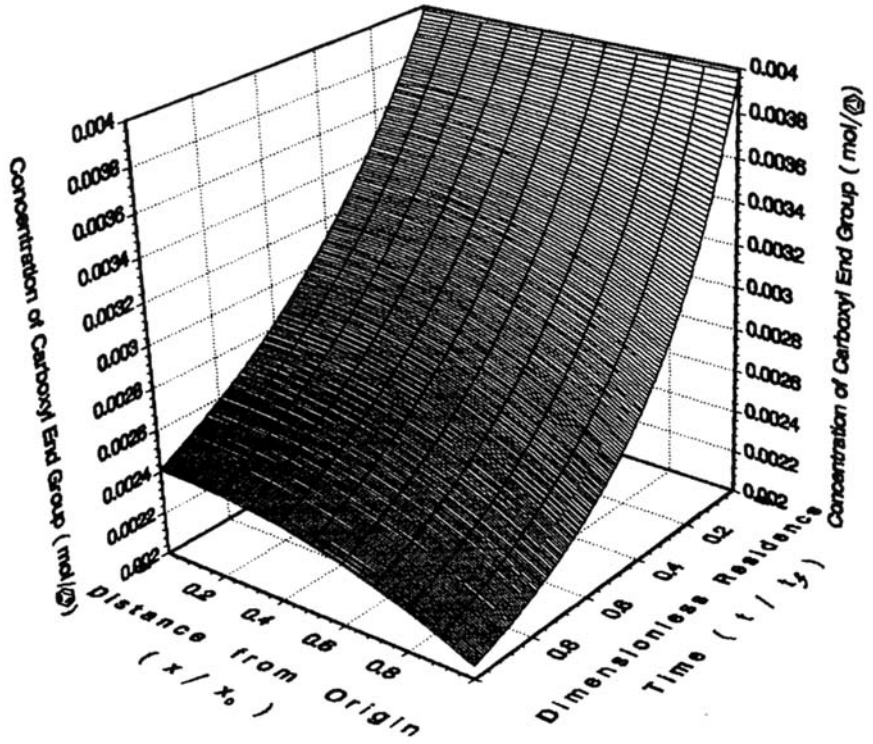

Figure 5 Internal distribution of carboxyl end group in a pellet during SSP at 225°C. The parameters are the same as those of curve 3 in Figure 2.

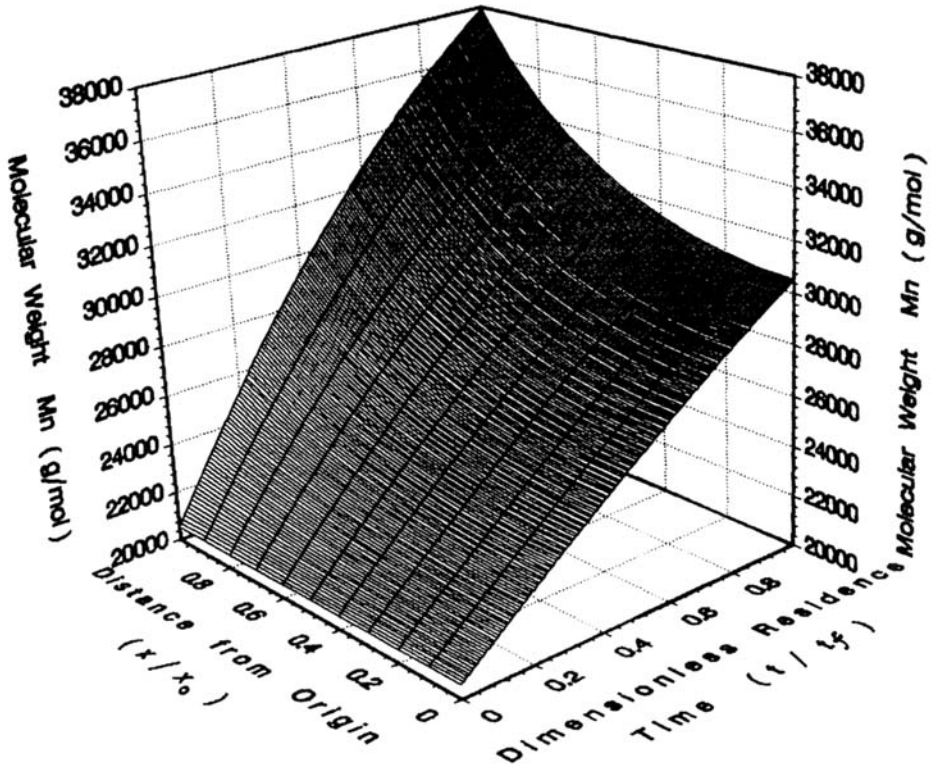

Figure 6 Internal distribution of molecular weight in a pellet during SSP at 225°C. The parameters are the same as those of curve 3 in Figure 2.

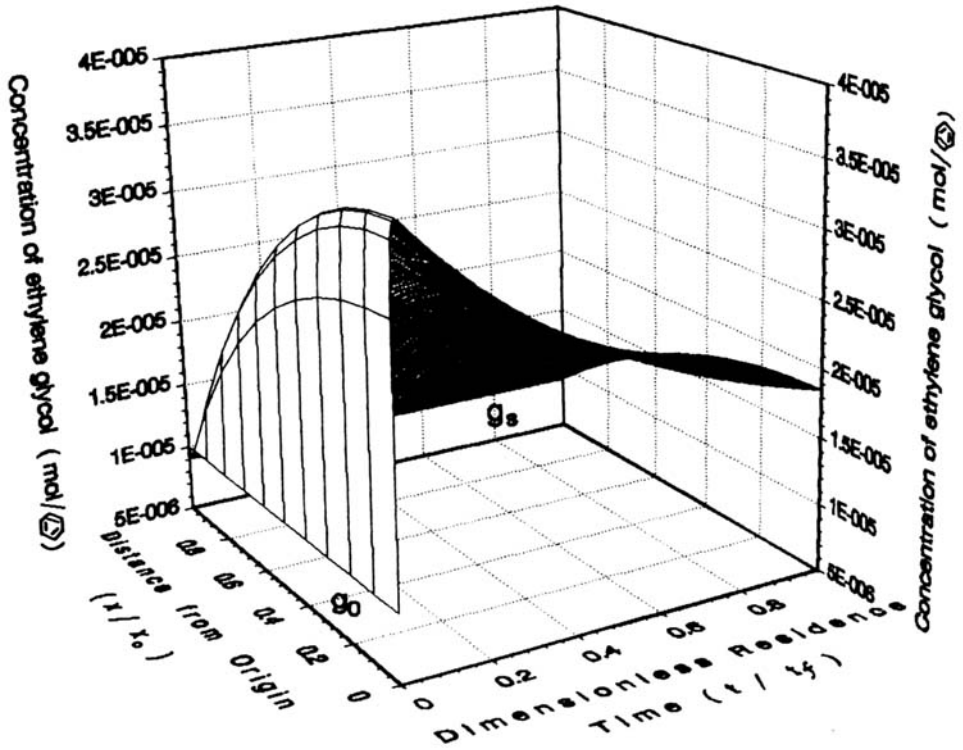

Figure 7 Internal distribution of ethylene glycol in a pellet during SSP at 225°C. The parameters are the same as those of curve 3 in Figure 2.

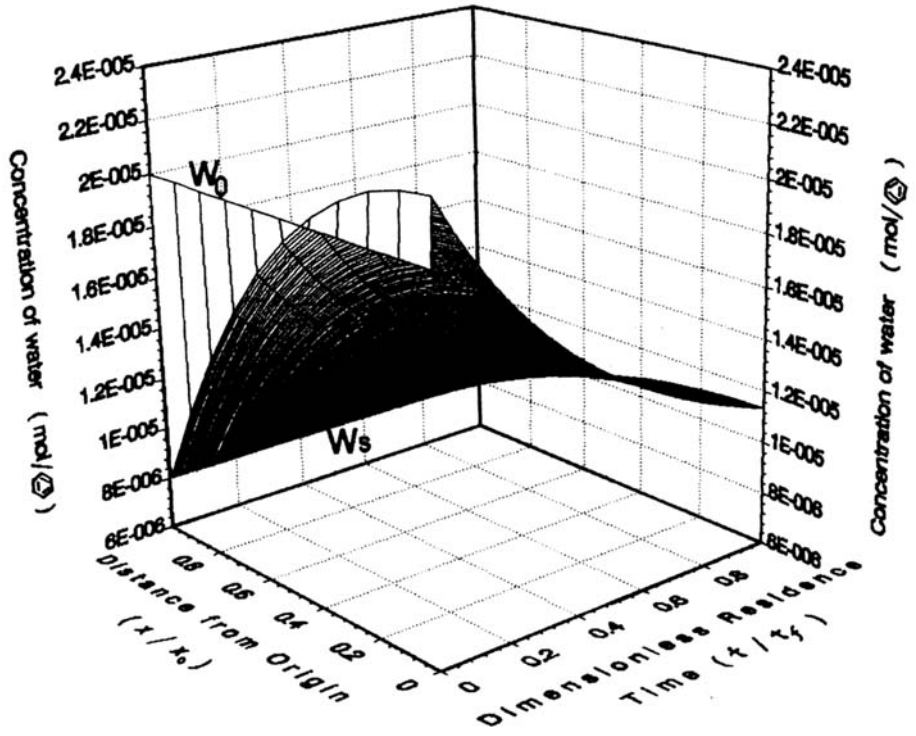

Figure 8 Internal distribution of water in a pellet during SSP at 225°C. The parameters are the same as those of curve 3 in Figure 2.

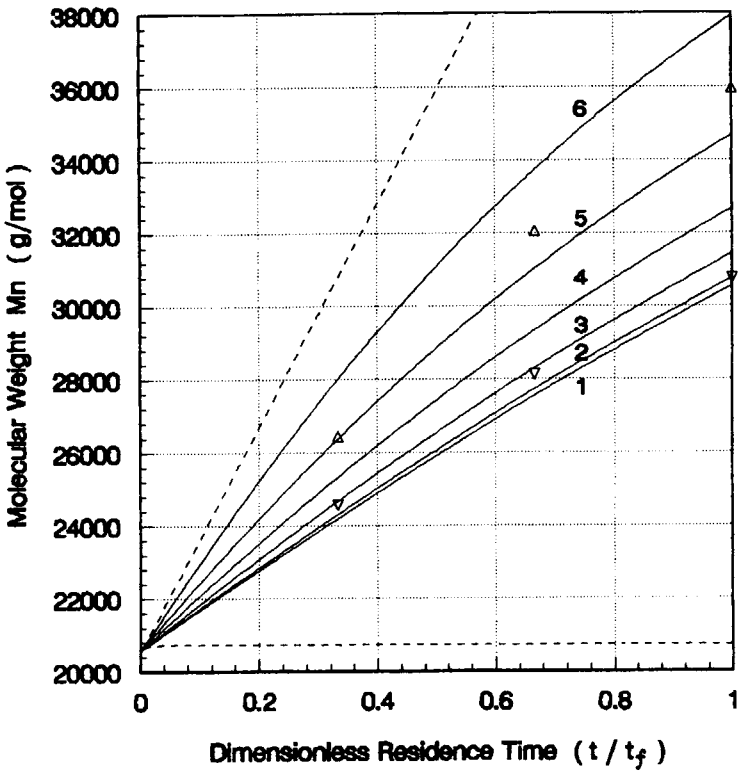

Figure 9 Local molecular weight vs. time during SSP at 225°C. Experimental data (△) and (▽) correspond to surface and center. Curves 1–6 between two broken lines correspond to $x = 0, 1/5x_o, 2/5x_o, 3/5x_o, 4/5x_o, x_o$. The parameters are the same as those of curve 3 in Figure 2.

tant to the assumption of $c_o = 0$, should be an expression without the appearance of rate constant k_1 in it.

In the case where k_1 is extremely large, so large that it guarantees the reaction to reach a new equilibrium instantly at the instantaneous removal of certain amount of EG, eq. (11) holds. Substituting its derivative into eq. (3) gives

$$\left(1 - \frac{1}{2K_1} + \frac{1 + g/2K_1}{\sqrt{4K_1 g + g^2}}\right)\frac{\partial g}{\partial t} = D_1 \frac{\partial^2 g}{\partial x^2}. \quad (36)$$

Solving eq. (36) for g, which is then substituted into eq. (11) to find e, followed by converting e to M_n, brings about a spate of curves in Fig. 11. Curves 5 and 6 above the broken line should mean that the extraordinarily high rate at the outer part of the pellet is unattainable. It is not surprising to witness such a futile occurrence because of the presumption of a drastic forward reaction rate constant. Usually, for polycondensation reactions, k_1 cannot be expected to be so large as to materialize the unique diffusion controlled process in SSP.

Gas Side Resistance

When the SSP is conducted in a fixed bed charged with pellets with heated dry nitrogen gas flowing through it, the assumption of $g_s = 0$, $w_s = 0$ is no longer feasible due to a gradual enrichment of EG and W content in the upward steam along the tube reactor. This is the reason we left the average g_s and w_s as independent parameters to be determined in data processing. In another event, the concentrations of EG and W in the bulk stream are invariably expressed in partial pressure (mm Hg), molar fraction, or molar concentration etc., but not in (mol/ ⬡) on the SSP reacting system base. The concentration conversion between the solid and gas phases should be ascribed to a phase equilibrium relation

$$g/P_g = A, \quad w/P_w = B \quad (37)$$

where, A and B are the global equilibrium constants for the adsorption of EG and W on the pellet from the inert gas, P_g and P_w are the partial pressures of EG and W in the bulk gas, g and w are the concentrations of EG and W in solid (mol/ ⬡).

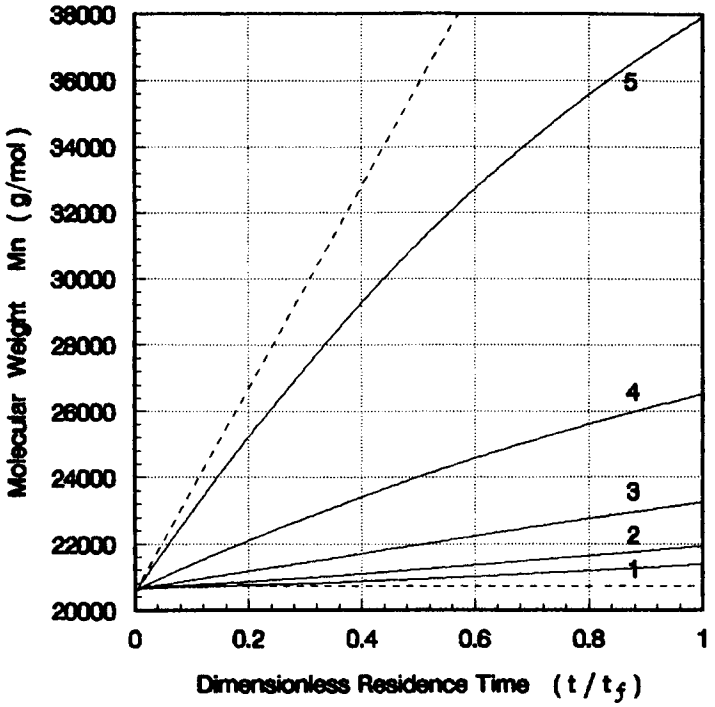

Figure 10 Local molecular weight vs. time during SSP at 225°C. Curves 1–5 between two broken lines correspond to $x = 1/5x_o$, $2/5x_o$, $3/5x_o$, $4/5x_o$, x_o, $x_o = 0.3$ cm. The other parameters are the same as those of curve 3 in Figure 2.

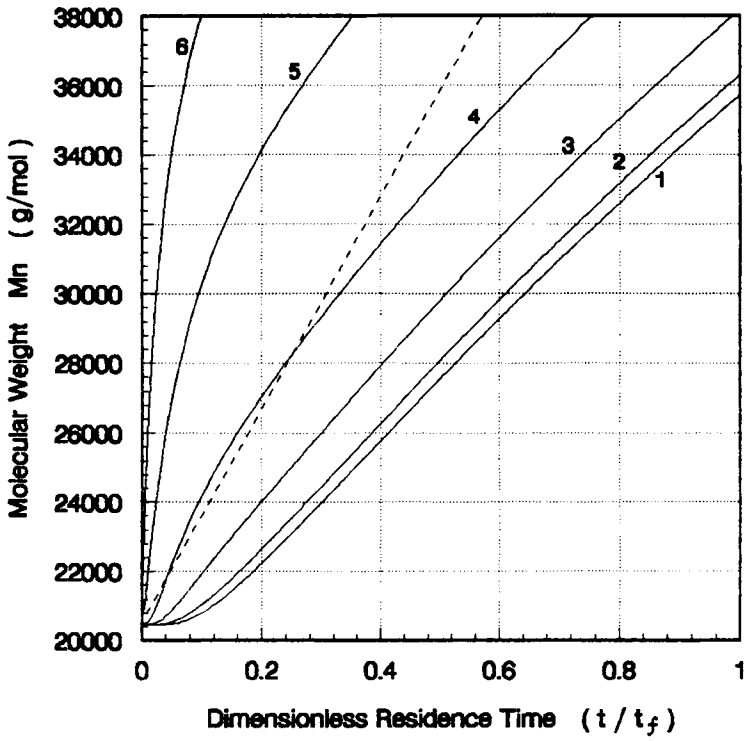

Figure 11 Local molecular weight vs. time in diffusion controlled process during SSP at 225°C. Curves 1–6 correspond to $x = 0$, $1/5x_o$, $2/5x_o$, $3/5x_o$, $4/5x_o$, $9/10x_o$, $e_o = 0.0187$, $c_o = 0$. The other parameters are the same as those of curve 3 in Figure 2.

When one takes into consideration the gas phase resistance, the boundary conditions in eq. (20) should be replaced by

$$-D_1 \frac{\partial g}{\partial x} = k_g(g - AP_g),$$

$$-D_2 \frac{\partial w}{\partial x} = k'_g(w - BP_w), \quad t > 0, \quad x = x_o, \quad (38)$$

in which, AP_g and BP_w are assumed to be the g_b and w_b in equilibrium with P_g and P_w.

There have been reports[10,15] that the polycondensation rate of SSP also depends on the types of inert gases, e.g., nitrogen, carbon dioxide, helium, etc., used in SSP. But the different influences on the molecular weight rise by different gases cannot be explained in terms of the variation of gas-side mass transfer coefficient resulting from the distinct diffusivity of each gas alone. For the same partial pressure of EG (or W) in the bulk streams of different inert gases, P_g will contribute differently to g_b due to the distinct value of A for each gas. Regardless, the complications associated with the realistic physicochemical interactions at the gas–solid interface, eq. (38), would be able to provide us with another phenomenological parameter, A, in analyzing the data of SSP with different inert gases.

CONCLUSIONS

A numerical method to seek a solution for the SSP process has been proposed to analyze the mechanism of SSP of PET. The parameters, D_1, D_2, k_1, k_2, g_s, and w_s were evaluated by collecting data in a fixed bed reactor. Results indicate that for the industrial SSP of PET, the overall reaction rate in a single pellet is appropriately simulated by a diffusion and reaction rate, jointly controlling model. From the core to the surface, SSP rate increases monotonically due to a gradual reduction of the concentration of by-products. However, the SSP rate at any location within the pellet is constrained between two purely reaction rate controlling cases. The unique diffusion controlling model is validated only in the case where the forward reaction rate constant is extremely large, but such a requirement can hardly be fulfilled for practical polycondensation reactions, including PET. Also presented in this work is a comment for the dependence of SSP rate on the types of inert gases. Taking into account the phase equilibrium of EG (and W) between the solid and different inert gases, we invoke another phenomenological parameter to distinguish the individual effect of one inert gas from the other.

The authors are grateful to the National United Chemical Engineering Laboratory, China, East China Institute of Chemical Technology, and Zhe Jiang University for its financial support.

NOMENCLATURE

c	concentration of carboxyl end groups (mol/⬡)
c_o	initial value of c (mol/⬡)
D_1	diffusivity of ethylene glycol (cm^2/s)
D_2	diffusivity of water (cm^2/s)
e	concentration of hydroxyl end groups (mol/⬡)
e_o	initial value of e (mol/⬡)
g	concentration of ethylene glycol (mol/⬡)
g_o	initial value of g (mol/⬡)
g_b	value of g in the bulk gas phase (mol/⬡)
g_s	value of g at the surface of the pellet (mol/⬡)
k_1	ester interchange reaction rate constant [$(mol/⬡)^{-1}\,h^{-1}$]
k_2	esterification reaction rate constant [$(mol/⬡)^{-1}\,h^{-1}$]
k_g	gas-side mass transfer coefficient (cm/s)
K_1	equilibrium constant of ester interchange reaction
K_2	equilibrium constant of esterification reaction
p	$= t/t_f$ dimensionless residence time
P_g	partial pressure of ethylene glycol in the bulk gas (mmHg)
P_w	partial pressure of water in the bulk gas (mmHg)
P_n	$= 2/(e + c)$ degree of polymerization
q	$= x/x_o$
t	reaction time (s)
t_f	total reaction time (s)
w	concentration of water (mol/⬡)
w_o	initial value of w (mol/⬡)
w_b	value of w in the bulk gas phase (mol/⬡)
w_s	value of w at the surface of the pellet (mol/⬡)
x	distance in the direction of diffusion (cm)
x_o	distance in the direction of diffusion from corn to surface of pellet (cm)
z	concentration of diester groups (mol/⬡)
z_o	initial value of z (mol/⬡)

REFERENCES

1. S. Chang, M. Sheu, and S. Chen, *J. Appl. Polym. Sci.*, **28,** 3289 (1983).
2. T. M. Chang, *Polym. Eng. Sci.*, **10,** 364 (1970).
3. E. Schaaf, H. Zimmermann, W. Dietzel, and P. Lohmann, *Acta Polym.*, **32,** 250 (1981).
4. F. C. Chen, R. G. Griskey, and G. H. Beyer, *AIChE J.*, **15,** 680 (1969).
5. K. Ravindranath and R. A. Mashelkar, *J. Appl. Polym. Sci.*, **39,** 1325 (1990).
6. H. Yokoyama, J. Sano, T. Chijiiwa, and R. Kajiya, *J. Jpn. Petrol. Inst.*, **21**(4), 271 (1978).
7. S. Chen and F. Chen, *J. Polym. Sci., Polym. Chem. Ed.*, **25,** 533 (1987).
8. A. Conix, *Makromol. Chem.*, **26,** 226 (1958).
9. H. Zimmermann, *Faserforsch.u.Textiltechnik,* **24,** 479 (1973).
10. H. Lichen, *J. Macromol. Sci. Phys.*, **B1**(4), 801 (1967).
11. G. Challa, *Makromol. Chem.*, **38,** 105 (1960).
12. S. K. Gupta and A. Kumer, *Reaction Engineering of Step Growth Polymerization,* Plenum Press, New York, 1987.
13. K. Ravindranath and R. A. Mashelkar, *J. Appl. Polym. Sci.*, **27,** 471 (1982).
14. B. D. Whitehead, *Ind. Eng. Chem. Proc. Des. Dev.*, **16,** 341 (1977).
15. R. M. Secor, *AIChE J.*, **15,** 861 (1969).

Received July 12, 1993
Accepted October 14, 1994